Results in Physics 8 (2018) 257–261

Contents lists available at ScienceDirect

Results in Physics

journal homepage: www.journals.elsevier.com/results-in-physics

Effect of the depth base along the vertical on the electrical parameters of a vertical parallel silicon solar cell in open and short circuit

Gokhan Sahin *, Genber Kerimli

Electric and Electronic Engineering Department, IĞDIR University, Iğdır 76000, Turkey

ARTICLE INFO

Article history:
Received 27 July 2017
Received in revised form 18 September 2017
Accepted 10 December 2017
Available online 14 December 2017

Keywords:
Depth base
Conversion efficiency
Electrical parameters
Open circuit
Short circuit

ABSTRACT

This article presented a modeling study of effect of the depth base initiating on vertical parallel silicon solar cell's photovoltaic conversion efficiency. After the resolution of the continuity equation of excess minority carriers, we calculated the electrical parameters such as the photocurrent density, the photovoltage, series resistance and shunt resistances, diffusion capacitance, electric power, fill factor and the photovoltaic conversion efficiency. We determined the maximum electric power, the operating point of the solar cell and photovoltaic conversion efficiency according to the depth z in the base. We showed that the photocurrent density decreases with the depth z. The photovoltage decreased when the depth base increases. Series and shunt resistances were deduced from electrical model and were influenced and the applied the depth base. The capacity decreased with the depth z of the base. We had studied the influence of the variation of the depth z on the electrical parameters in the base.

Introduction

Solar cell is the device that allows the direct conversion of sunlight to electricity. This conversion process is based on excess minority carrier's collection leading to a current flow but this carriers collection is perturbed by recombination phenomena. That is why many studies [1–6] have been made on solar cells to improve the conversion efficiency. Photovoltaic (PV) systems generate green energy with no pollution and have a long life time. In the past, the energy photovoltaic conversion efficiency of PV modules was 10%–14% [7]. Recently, efficiency has been increased to 15%–22% in commercially available PV modules and a research laboratory reported that the efficiency of solar cells is up to 44.7% [8].

The purpose of this article is to do a study on a parallel vertical junction silicon solar cell under multispectral illumination in static regime [9]. A theoretical study of the excess minority carriers in the base of the solar cell is produced through continuity equation. With help of the boundary conditions at the junction and at the middle of the base, excess minority carriers density are studied and lead to the expression of photocurrent density and photovoltage. From, the well-known I-V characteristic of the solar cell under illumination, electrical equivalent model is established for low and high junction recombination values giving respectively ideal generator source of tension and current. The present work can be allowing a measurement of the parasitic resistances (series and shunt resistance) and effect of the depth base on the electrical parameters of a parallel vertical junction solar cell under polychromatic illumination [10].

The aims of this article we studied modeling of the influence of the depth z on the vertical parallel silicon solar cell's photovoltaic conversion efficiency. From the diffusion-recombination equation the excess minority carrier's density, the photocurrent density and the photovoltage will be determined. In the last part of this work we calculated the solar cell photovoltaic conversion efficiency and our simulation results.

Theory

For these types of solar cells, the bases are connected to each other and the emitters to each other. Each base is framed by two junctions as well as the transmitters. The solar rays fall on the cell parallel to the junction. We present on Fig. 1 a unit cell of a vertical junction's silicon solar cell under various wavelengths. H is the base width, θ is the illumination incidence angle and x is the depth in the base [11,12].

To understand the functioning of such a structure, we will extract from this network an elementary cell or basic cell which we present in Fig. 2.

The contribution of the base to the photocurrent is larger than that of the emitter [13] and our analysis will only be developed in the base region. Taking into account the generation, recombina-

* Corresponding author.
E-mail address: gokhan.sahin@igdir.edu.tr (G. Sahin).

https://doi.org/10.1016/j.rinp.2017.12.021
2211-3797/© 2017 The Authors. Published by Elsevier B.V.

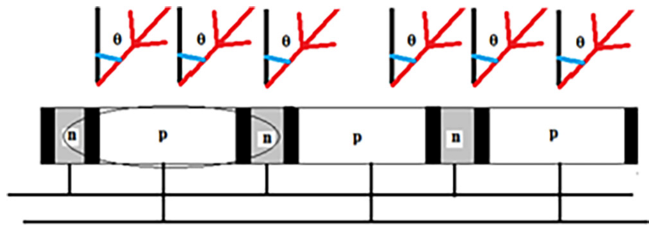

Fig. 1. Vertical parallel junction silicon solar cell.

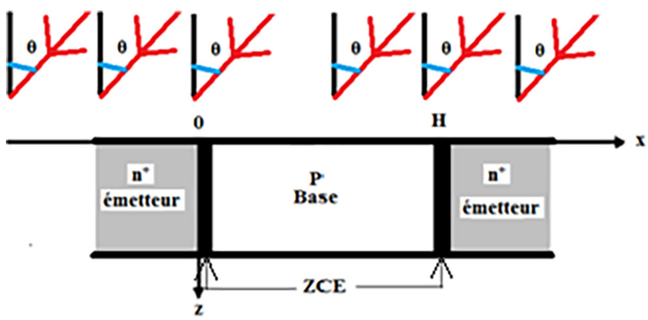

Fig. 2. Diagram of solar cell in parallel vertical junction in the base.

tion and diffusion phenomena in the base, the equation governing the variation of the minority carriers density δ(x,y,z,t) under modulation frequency is:

$$D(\omega)\cdot\frac{\partial^2\delta(x,\theta,z,t)}{\partial x^2}-\frac{\delta(x,\theta,z,t)}{\tau}=-G(z,\theta,t)+\frac{\partial\delta(x,\theta,z,t)}{\partial t} \quad (1)$$

D(ω) [14] and τ are respectively, the excess minority carrier diffusion constant and lifetime.

The excess minority carriers' density can be written as:

$$\delta(x,t)=\delta(x)\exp(-j\omega t) \quad (2)$$

Carrier generation rate G (z, θ, t) is given by:

$$G(z,\theta,\lambda,t)=g(z,\theta,\lambda)\times\exp(-j\omega t) \quad (3)$$

where

$$g(z,\theta,\lambda)=\alpha(\lambda)(1-R(\lambda))\times\phi(\lambda)\times\exp(-\alpha(\lambda)\times z)\times\cos(\theta) \quad (4)$$

ω is the angular frequency, θ is the incidence angle, z the base depth according to the vertical axis; Sf is the junction recombination velocity and λ the illumination wavelength.

If we replace Eq. (2) into Eq. (1), the temporary part is eliminated and we obtain:

$$\frac{\partial^2\delta(x)}{\partial x^2}-\frac{\delta(x,\theta,z,t)}{L(\omega)^2}=-\frac{g(z,\theta)}{D(\omega)} \quad (5)$$

The solution of this equation is:

$$\delta(x,\omega,\theta,z,Sf,\lambda)=A\cosh\left(\frac{x}{L(\omega)}\right)+B\sinh\left(\frac{x}{L(\omega)}\right)+\frac{L(\omega)^2}{D(\omega)}\cdot\alpha(\lambda)(1-R(\lambda))\cdot\phi(\lambda)\cdot\exp(\alpha(\lambda)\cdot z)\cdot\cos(\theta) \quad (6)$$

Coefficients A and B are determined through the following boundary conditions [15]:

– at the junction (x = 0):

$$D(\omega)\cdot\left.\frac{\partial\delta(x,\omega,\theta,z)}{\partial x}\right|_{x=0}=Sf\cdot\delta(x,\omega,\theta,z)|_{x=0} \quad (7)$$

Sf is the excess minority carrier's recombination velocity at each junction [16].

– at the middle of the base (x = H/2):

$$D(\omega)\cdot\left.\frac{\partial\delta(x,\omega,\theta,z)}{\partial x}\right|_{x=\frac{H}{2}}=0 \quad (8)$$

Results and discussion

The excess minority carriers density

In this section, we will study the density of minority carriers generated in the base. It will show the effect of, vertical depth, on the profile of the density of the load carriers as a function of the depth in the base. Fig. 3 represents the variation of the minority carriers density in the base versus thickness x for various depth z.

On Fig. 3, the excess minority carriers density in the base increases to reach a maximum corresponding to the thickness x_o in the base, but it decreases for a depth (z) x > x_o. It also decreases in amplitude as a function of the depth according to the vertical of the illumination. From this remark, we distinguish three zones:

- a first zone 0 ≤ x ≤ x_o; the gradient of the excess minority carriers' density in the base of the photovoltaic cell is positive: this corresponds to the passage of an electron flux causing a photocurrent through the emitter-base junction,
- a second zone: x = x_o; The modulus of the excess minority carrier's density in the base is maximal and the gradient is zero, so there is a storage of excess minority carrier's density negative charges which will create a variation of the space charge area which extends from the junction to the value x_o,
- a third zone: x_o ≤ x ≤ H; The modulus of excess minority carrier's density decreases in the base, thus implying a negative gradient.

We note that as one enters the base z, the density of the minority carrier's decreases. Indeed, the variation of the density of the minority carrier's according to depth (z), is governed by the rate of generation which follows a Beer Lambert law: an exponential decay as one penetrates inwards. This situation predicts the capacitive phenomena evolution.

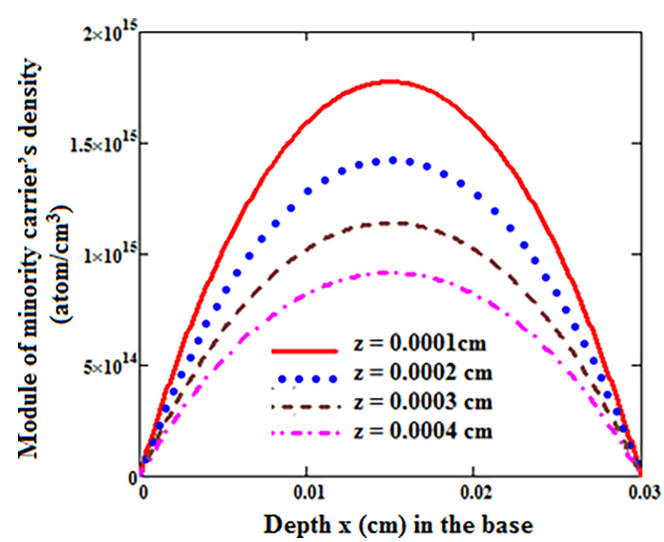

Fig. 3. Module of minority carrier's density versus thickness x in the base for various depth z, Sf = 3.10^3 cm/s. H = 0.03 cm; L_o = 0.02 cm, D_o = 26 cm^2/s, θ = 20^0, λ = 0.52 μm, ω = 10^3 rad/s.

Photocurrent density

In this section, we make a study in modeling the density of photocurrent delivered by the base of the photovoltaic. This photocurrent is due to the diffusion of electrons through the base of the photovoltaic cell. The excess minority carriers in the base will flow across the two junctions (emitter1-first half of the base and emitter 2-s half of the base) by diffusion (Fig. 2) The photocurrent density is given by the following expression [11–13,17,18]:

$$J_{Ph} = 2 \cdot q \cdot D(\omega) \cdot \left.\frac{\partial\delta(x,\omega,\theta)}{\partial x}\right|_{x=0} \quad (9)$$

were q is the elementary charge.

On Fig. 4 we represent the profile of the photocurrent density as a function of the logarithm of the modulation frequency for various depths (z) along the vertical and on Fig. 5 the photocurrent of short-circuit versus the depth base.

It is still observed that the photocurrent density is maximum and hardly varies for the low frequencies and corresponding to photocurrent of the short-circuit. Then a sudden decrease is observed until the photocurrent density is canceled with the increase of the modulation frequency. Fig. 4 shows a decrease in the amplitude of the photocurrent density with the depth along the vertical. This can be explained by the fact that with depth there is the attenuation of the wave as predicted by BEER LAMBET's law. To low values of the logarithm of the modulation frequency, the photocurrent density is almost nonexistent representing the situation of open circuit of the solar cell. The photogenerated carriers are thus blocked to the junction. The solar cell operates in situation of short-circuit, where the maximum of carriers cross the junctions to be part of the photocurrent. This figure shows again the decreasing of the photocurrent density of short-circuit when we go in depth, which is illustrated at Fig. 5.

Photovoltage

When the photovoltage is illuminated, there is generation of minority carriers by photoelectric effect giving rise to a surface potential in the semiconductor obtained by illuminating an energy greater than the gap of the semiconductor and the photogenic carriers being separated by a Electric field intense in the space charge

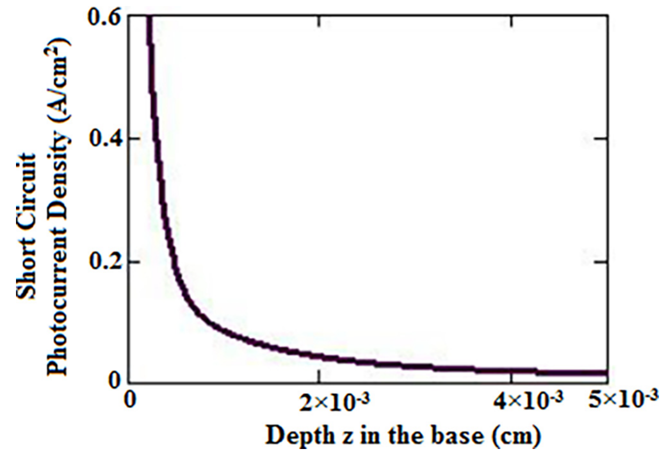

Fig. 5. Short circuit photocurrent density versus the depth z. Sf = 3.10^3 cm/s; H = 0.03 cm; L_o = 0.02 cm; D_o = 26 cm^2/s; θ = 20°; λ = 0.52 μm.

area at the surface. The voltage obtained at the solar cell terminals will now be called photovoltage. Based on the excess minority carrier's density, we can determine the photovoltage across the junction, according to the Boltzmann's relation, as inutile [11,17,19,20].

$$V_{ph} = V_T \cdot \ln\left[1 + \frac{Nb}{n_0^2} \cdot \delta(0)\right] \quad (10)$$

with

$$V_T = \frac{K \cdot T}{q} \quad (11)$$

V_T the thermal voltage, Nb the base doping density, n_0 the intrinsic carriers' density, K is the Boltzmann constant; T is the absolute temperature and q is the elementary charge of the electron.

The phototension will be studied first as a function of the frequency, then as a function of the logarithm of the depth z [11–15,21,22]. We represent in Fig. 6 the profile of the phototension as a function of the logarithm of the modulation frequency ω for different depths (z) along the vertical and on Fig. 7 the photocurrent of short-circuit versus the depth z.

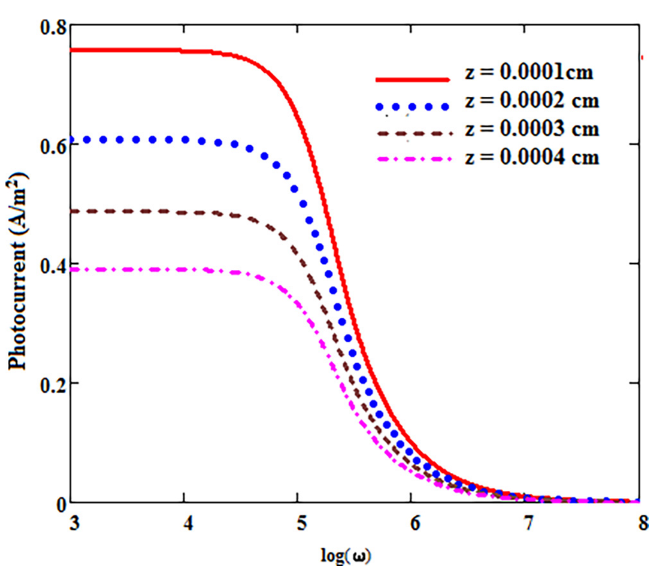

Fig. 4. Photocurrent density versus logarithm of the modulation frequency log(ω) for various depth z. Sf = 3.10^3 cm/s; H = 0.03 cm; L_o = 0.02 cm; D_o = 26 cm^2/s; θ = 20°; λ = 0.52 μm.

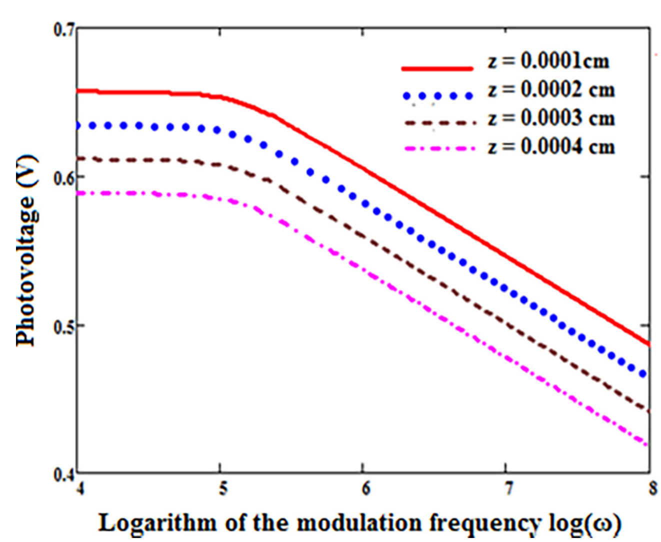

Fig. 6. Photovoltage versus logarithm of the modulation frequency log(ω) for various depth z in the base. Sf = 3.10^3 cm/s; H = 0.03 cm; L_o = 0.02 cm; D_o = 26 cm^2/s; θ = 20°; λ = 0.52 μm.

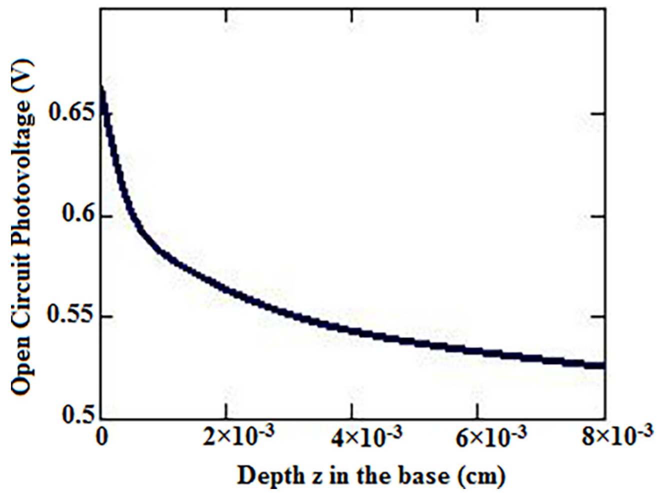

Fig. 7. Open circuit photovoltage versus depth z in the base. Sf = 3.10^3 cm/s; H = 0.03 cm; L_o = 0.02 cm; D_o = 26 cm^2/s; θ = 20°; λ = 0.52 μm.

The photovoltage always maintains a maximum step before gradually decreasing to a low value. Fig. 6 shows the behavior of the photovoltage as a function of the logarithm of the frequency remains identical to that studied on the effect of the depth z in the base.

More than the depth (z) in the base along the vertical is high the less the photovoltage. Indeed, the wave arrives at depth of its deprived exciting energy. Added to that there, the rigidity and the defects of construction in depth one do not allow a good mobility of the carriers. For the great values of the logarithm of the modulation frequency, the carriers manage to traverse the junction involving thereafter the considerable fall of the photovoltage. When we advance in the depth, the carriers number decreases. We can notice the reduction in the open circuit photovoltage confirms in Fig. 7.

Photovoltaic conversion efficiency

When the solar cell is illuminated, it produces electricity thanks to the photovoltaic effect. This photovoltaic cell delivers a DC voltage. It is therefore possible to measure the power delivered by the photovoltaic cell and to compare it with the efficiency of a reference cell. The photovoltaic conversion efficiency is given by the Eq. (12) [15]:

$$\eta(\omega, \theta, z, Sf, \lambda) = \frac{P\max(\omega, \theta, z, Sf, \lambda)}{P_{inc}} \quad (12)$$

where P (ω, θ, z, Sf, λ) is the power per unit area delivered by the photovoltaic cell and P_{inc} is the power of the incident wave under AM 1.5 and taken equal to 100 mW/cm^2. The profile of the conversion efficiency as a function of junction recombination velocity for different depths z is shown in Fig. 8.

The Conversion efficiency of profile (Fig. 8) always shows an upward slope to the maximum efficiency and then a downward slope above this maximum. The conversion efficiency decreases with increasing depth z. Indeed it is the law of Beer Lambert that governs the behavior of the wave once the wave is emitted [23–25]. We present in Table 1 some optimal efficiency values for different depths along z.

Table 1 and Fig. 9 shows the decreases of conversion efficiency with depth z increases in the base.

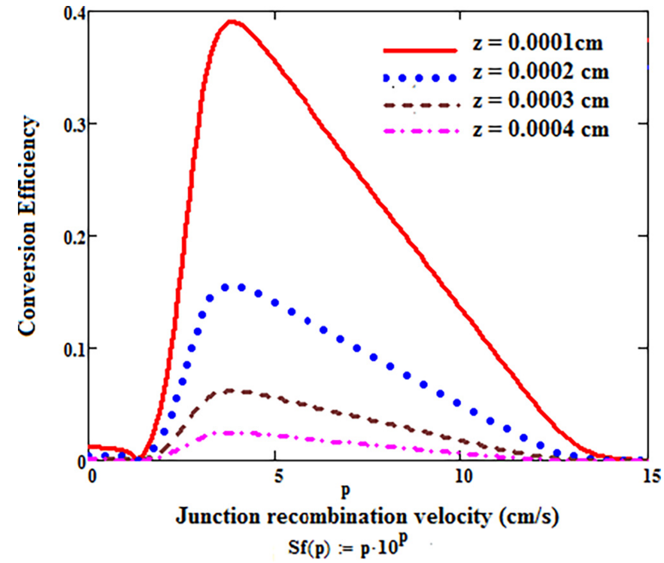

Fig. 8. Module of the conversion efficiency of the photovoltaic material versus junction recombination velocity for different depths in the base. λ = 0.52 μm, H = 0.03 cm, L_o = 0.02 cm, D_o = 26 cm^2/s, θ = 20°, ω = 10^3 rad/s.

Table 1
Values of optimum conversion efficiency of the photovoltaic material for different depths along the vertical z at the junction recombination velocity Sf = 3098.10^4 cm/s.

z (cm)	0.0001	0.0002	0.0003	0.0004
η	0.39	0.155	0.062	0.025

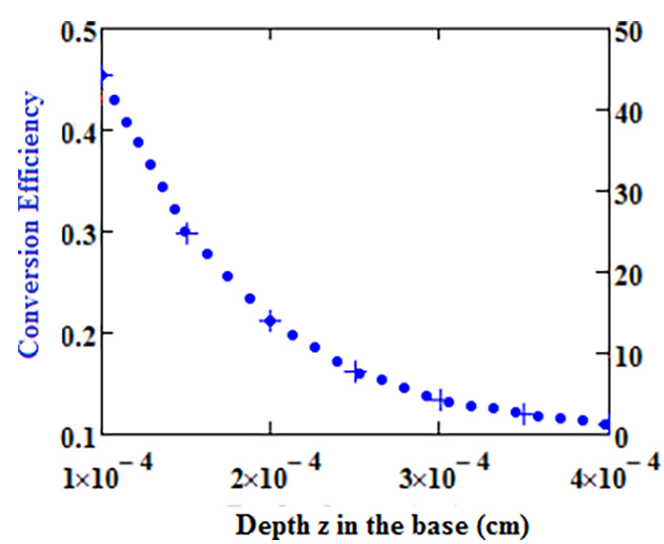

Fig. 9. Evolution of the conversion efficiency versus depth z in the base. H = 0.03 cm, L_o = 0.02 cm, D_o = 26 cm^2/s, ω = 10^3 rad/s, θ = 20°, z = 0.0001 cm, λ = 0.52 μm.

Conclusion

In this article we made a theoretical study of a junction vertical parallel silicon solar cell under polychromatic illumination. The resolution of the continuity equation allowed us to establish the expression of excess minority carrier charge density in the base of the solar cell. The study showed that when the depth z increases the minority carriers density as well as the electrical parameters such as the photocurrent density, the photovoltage and conversion efficiency decrease because of attenuation of the incident light. The effect on some electrical quantities was studied. The study was done in the visible range. Our computed results have shown that the performance of solar cell is junction recombination velocity and conversion efficiency reaches about 38%.

Appendix A. Supplementary data

Supplementary data associated with this article can be found, in the online version, at https://doi.org/10.1016/j.rinp.2017.12.021.

References

[1] Neamen DA. Semi-conductor physics and devices basic principle. New York: McGraw-Hill; 2003.

[2] Sinton RA, Swanson PM. An optimisation study of Si Point Contact Concentration. In: 15th I.E.E.E. Photov. Spect. Conf. USA; 1987. p. 1207–08.

[3] Thongpron J, Kirtikara K, Jivacate C. Sol Energy Mater Solar Cells 2006;90:3078–84.

[4] Topkaya R. Ferromagnetic resonance study of Fe/Cu multilayer thin film. J Supercond Nov Magn 2017;30(5):1275–80.

[5] Orton JW, Blood P. The electrical characterization of semiconductors: measurement of minority carrier properties. London: Academic Press; 1990.

[6] Zondervan A, Verhoef LA, Lindholm FA. Measurement circuits for silicon-diode and solar-cell lifetime and surface recombination velocity by electrical short-circuit current decay. IEEE Trans Electron Dev 1988;35:85–8.

[7] Rauschenbach HS. Solar cell array design handbook, Vol. 1. JPL, Pasadena, CA, USA: Van Nostrand Reinhold; 1976.

[8] Wenham SR, Green MA, Watt ME, Corkish R. Applied photovoltaics. 2nd ed. ARC, Centre for Advanced Silicon Photovoltaics and Photonics; 2007.

[9] Bordin N, Kreinin L, Eisenberg N. Determination of recombination parameters of bifacial silicon cells with a two layer step-liked effect distribution in the base region. In: Proc.17th European PVSEC, Munich; 2001.p. 1495–98.

[10] Bensalem S, Chegaar M. Thermal behavior of parasitic resistances of polycrystalline silicon solar cells. Revue des Energies Renouvelables 2013;16:171–6.

[11] Şahin G. Effect of incidence angle on the electrical parameters of vertical parallel junction silicon solar cell under frequency domain. Moscow Univ Phys Bull 2016;71(5):498–507. ISSN 0027-1349.

[12] Şahin G. Effect of junction recombination velocity of electrical parameters of a vertical parallel silicon solar cell under frequency modulation. Appl Phys A 2016;122:997. https://doi.org/10.1007/s00339-016-0506-9.

[13] Şahin G. Effect of wavelength on the electrical parameters of a vertical parallel junction silicon solar cell illuminated by its rear side in frequency domain. Results Phys 2016;6:107–11.

[14] Diallo HL, Wereme A, Maiga AS, Sissoko G. New approach of both junction and back surface recombination velocities in a 3D modelling study of a polycrystalline silicon solar cell. Eur Phys J Appl Phys 2008;42:203–11.

[15] Diallo HL, Dieng B, Ly I, Dione MM, Ndiaye M, Lemrabott OH, et al. Determination of the recombination and electrical parameters of a vertical multijunction silicon solar cell. Res J Appl Sci Maxwell Sci Organ 2012;4 (16):2626–31.

[16] Avraham Gover, Paul Stella. Vertical multijunction solar-cell one-dimensional analysis. IEEE Trans Electron Dev 1974;21(6):351–6.

[17] Ndiaye EH, Sahin G, Dieng M, Thiam A, Diallo HL, Ndiaye M, Sissoko G. Study of the intrinsic recombination velocity at the junction of silicon solar under frequency modulation and irradiation. J Appl Math Phys 2015;3:1522–35. https://doi.org/10.4236/jamp.2015.

[18] Sane M, Zoungrana M, Diallo HL, Sahin G, Thiam N, Ndiaye M, et al. Int J Invent Eng Sci 2013;1(11):37.

[19] Dieme Nfally. Study of the electrons density in the base of the parallel vertical junction solar cell under the influence of the temperature. Am J Opt Photon 2015;3(1):13–6.

[20] Sane M, Sahin G, Barro FI, Seidou MA. Incidence angle and spectral effects on vertical junction silicon solar cell capacitance. Turk J Phys 2014;38:221–7. https://doi.org/10.3906/fiz-1311-9.

[21] Mathieu H, Fanet H. 'Physique des semiconducteurs et des composants électroniques. 6ème Ed. Dunod; 2009.

[22] Sahin G, Dieng M, Ould EMMA, Ngom MI, Thiam A, Sissoko G. Capacitance of vertical parallel junction silicon solar cell under monochromatic modulated illumination. J Appl Math Phys 2015;3:1536–43. https://doi.org/10.4236/jamp.2015.311178.

[23] Sonntag P, Preissler N, Bokalič M, Trahms M, Haschke J, Schlatmann R, et al. Silicon solar cells on glass with power conversion efficiency above 13% at thickness below 15 micrometer. Sci Rep 2017;7(1):873. https://doi.org/10.1038/s41598-017-00988-x.

[24] Grigoryev DV, Lozovoy KA, Pishchagin AA. Analysis of efficiency of solar energy conversion by tandem CdxZn1-xTe/Si solar cell. J Phys Conf Ser 2014;541:012048.

[25] Chen Yen-Chi, Chen Teng-Ming. Improvement of conversion efficiency of silicon solar cells using up-conversion molybdate $La_2Mo_2O_9$:Yb, R (R = Er, Ho) phosphors. J Rare Earths 2011;29(8):723.